frontiers in Immunology

TYPE Original Research
PUBLISHED 03 November 2026
DOI 10.3389/fimmu.2026.1875198

Check for updates

OPEN ACCESS

EDITED BY
Yongbo Kang,
Shanxi Medical University, China

REVIEWED BY
Tsunehiko Maruyama,
Mito Saiseikai General Hospital, Japan
Yu Zhang,
Mianyang Third People's Hospital, China

*CORRESPONDENCE
Zhiqiang Wang
zhi_qiang_wang123@163.com

RECEIVED 07 May 2026
REVISED 11 October 2026
ACCEPTED 19 October 2026
PUBLISHED 03 November 2026

CITATION
Wang Z, Zheng J, Wang L, Meng N, Guo H, Shi Y, Xu W and Yang P (2026) A pretreatment hormonal-nutritional-immune score for locally advanced gastric cancer receiving neoadjuvant immunochemotherapy: a multicenter retrospective cohort study. *Front. Immunol.* 17:1875198. doi: 10.3389/fimmu.2026.1875198

COPYRIGHT
© 2026 Wang, Zheng, Wang, Meng, Guo, Shi, Xu and Yang. This is an open-access article distributed under the terms of the Creative Commons Attribution License (CC BY). The use, distribution or reproduction in other forums is permitted, provided the original author(s) and the copyright owner(s) are credited and that the original publication in this journal is cited, in accordance with accepted academic practice. No use, distribution or reproduction is permitted which does not comply with these terms.

A pretreatment hormonal-nutritional-immune score for locally advanced gastric cancer receiving neoadjuvant immunochemotherapy: a multicenter retrospective cohort study

Zhiqiang Wang[1]*, Jie Zheng[2], Le Wang[1], Ning Meng[1], Honghai Guo[3], Yanlong Shi[4], Wen Xu[5] and Peigang Yang[3]

[1]Department of Gastrointestinal Surgery, Shijiazhuang People's Hospital, Shijiazhuang, Hebei, China, [2]Department of Ultrasound, Shijiazhuang People's Hospital, Shijiazhuang, Hebei, China, [3]The Third Department of Surgery, The Fourth Hospital of Hebei Medical University, Shijiazhuang, Hebei, China, [4]Department of General Surgery, The Fifth Affiliated Hospital of Anhui Medical University, Hefei, Anhui, China, [5]Department of Medical Record, Yichang Central People's Hospital, Yichang, Hubei, China

Background: Pathological response and survival following neoadjuvant PD-1 inhibitor plus chemotherapy in locally advanced gastric cancer (LAGC) are heterogeneous, and tumor biomarkers do not capture host endocrine, nutritional, or inflammatory status. We developed a pretreatment Hormonal-Nutritional-Immune Score (HNIS) based on 12 routine blood indicators.

Methods: This multicenter retrospective cohort enrolled 342 patients with cT2-4bN_anyM0 gastric or gastroesophageal junction (GEJ) adenocarcinoma treated with at least 2 cycles of PD-1 inhibitor plus platinum-based chemotherapy at 4 Chinese centers between December 2019 and January 2023, with patients allocated to a training cohort (n=206), an internal validation cohort (n=68), and an external validation cohort (n=68). HNIS assigned 1 point for each of 12 hormonal, nutritional, and inflammatory abnormalities; patients were stratified as Low (0 to 2), Intermediate (3 to 5), or High risk (6 or greater). The primary endpoint was major pathological response (MPR). Logistic regression, Cox regression, Kaplan-Meier analysis, and discrimination analyses were used. Additional analyses assessed treatment interactions, individual components, LASSO-derived weights, and alternative group boundaries using repeated nested cross-validation.

Results: The median age was 62 years, 233 patients (68.1%) were male, and the median HNIS was 3 (IQR 2 to 5); 138 (40.4%) were Low risk, 121 (35.4%) Intermediate, and 83 (24.3%) High risk. MPR rates declined from 67.4% in Low risk to 46.3% in Intermediate and 20.5% in High risk patients (P<0.001), and grade 3 or higher immune-related adverse events (irAEs) increased from 7.2% to 9.9% to 26.5% (P<0.001). Each one-point HNIS increase was independently associated with lower odds of MPR (adjusted OR 0.68, 95% CI 0.61 to 0.76; P<0.001). At a median follow-up of 52.5 months, 3-year DFS was 69.6%, 58.7%, and 24.1%, and 3-year OS was 94.9%, 87.6%, and 69.9% across the 3 groups (both log-rank P<0.001). The HNIS score achieved AUCs of 0.725, 0.736, and 0.753 for MPR

prediction in the training, internal, and external validation cohorts, outperforming a clinical model based on stage, PD-L1, and MMR (AUCs 0.554 to 0.611; DeLong all P<0.05). In supplementary repeated cross-validation, the equal-weight score had an AUC of 0.733, compared with 0.704 for a nine-component LASSO model. **Conclusions:** A pretreatment HNIS based on routine blood tests independently predicts MPR, severe irAEs, DFS, and OS in patients with LAGC receiving neoadjuvant PD-1 inhibitor plus chemotherapy, and may refine pretreatment risk stratification beyond conventional staging and tumor biomarkers.

KEYWORDS

gastric cancer, gastroesophageal junction adenocarcinoma, hormonal-nutritional-immune score, immune-related adverse events, neoadjuvant immunotherapy, pathological response, PD-1 inhibitor

Introduction

Gastric cancer is the fifth most commonly diagnosed malignancy and the fourth leading cause of cancer-related death worldwide, accounting for approximately 1.09 million new cases and 769,000 deaths in 2020 (1). In China, more than half of patients present with locally advanced disease (LAGC, defined here as clinical stage cT2-4bN_anyM0), at which point upfront resection alone is associated with high relapse rates (2). Gastric and gastroesophageal junction (GEJ) adenocarcinomas are managed using multimodal strategies that integrate systemic therapy and surgery (3). Perioperative platinum-based chemotherapy has improved resection rates and overall survival, but recurrence remains common (4, 5).

Immune checkpoint inhibitors (ICIs) targeting the PD-1/PD-L1 axis have been incorporated into neoadjuvant regimens for LAGC and GEJ adenocarcinoma. DANTE, MATTERHORN, and KEYNOTE-585 evaluated perioperative chemotherapy combined with PD-L1 blockade (atezolizumab or durvalumab) or PD-1 blockade (pembrolizumab) and reported increased pathological complete response (pCR) rates relative to chemotherapy alone (6–8). Histopathological tumor regression is associated with prognosis after neoadjuvant chemotherapy; this association does not by itself establish pCR or major pathological response (MPR) as validated surrogates for survival (9). However, only a subset of patients achieve pCR or MPR, and the same regimen may produce markedly different immune-related toxicity profiles, ranging from absence of clinically relevant events to grade ≥3 events that interfere with surgical timing or curative-intent treatment intent.

Tumor-derived biomarkers, including PD-L1 combined positive score (CPS) and microsatellite-instability-high/mismatch repair-deficient (MSI-H/dMMR) status, can inform immunotherapy selection in advanced gastric cancer, but do not directly characterize host endocrine, nutritional, or inflammatory status (10, 11). Recent multicenter and AI-assisted studies in Chinese cohorts have integrated imaging, pathological, and clinical information to predict occult peritoneal disease or postoperative recurrence (12–15), but no inexpensive systemic biomarker has yet entered routine clinical practice for neoadjuvant immunotherapy decision-making.

Antitumor immunity depends on coordinated T-cell activation, antigen presentation, cytokine signaling, metabolic fitness, and adequate host nutritional reserve (16, 17). Hormonal axes also influence immunotherapy response and toxicity. Thyroid dysfunction is a recognized immune-related adverse event (irAE) during PD-1 blockade (18). Stress-axis activation and elevated glucocorticoid tone can suppress dendritic-cell maturation and T-cell priming (19). On the metabolic side, the triglyceride-glucose (TyG) index is a surrogate of insulin resistance and has been examined in advanced gastric cancer treated with immunotherapy plus chemotherapy (20). Serum albumin and the prognostic nutritional index (PNI), which incorporates albumin and lymphocyte count, characterize aspects of nutritional status and have been associated with clinical outcomes in gastrointestinal cancer (21, 22). The neutrophil-to-lymphocyte ratio (NLR), systemic immune-inflammation index (SII), CRP, and the CRP-to-albumin ratio (CAR) summarize peripheral inflammatory abnormalities and have been associated with cancer prognosis (23–26).

Despite extensive work on individual biomarkers, no integrated, low-cost, blood-based pretreatment composite covering all three axes (hormonal, nutritional, and inflammatory) has been validated in the perioperative ICI setting for LAGC. We therefore designed a Hormonal-Nutritional-Immune Score (HNIS), summing 12 binary pretreatment laboratory indicators across the three domains, and evaluated its prognostic and predictive performance in a multicenter retrospective cohort of 342 patients with LAGC treated with neoadjuvant PD-1 inhibitor plus platinum-based chemotherapy. We aimed to: (i) characterize the distribution of HNIS across training, internal validation, and external validation cohorts; (ii) test the association between HNIS and MPR, pCR, and overall response; (iii) characterize the relationship between HNIS and irAEs (any grade and grade 3 or higher); (iv) assess HNIS as an independent predictor of DFS and OS; and (v) compare the discrimination and calibration of HNIS-based prediction with a conventional clinical staging-based model.

Materials and methods

Study design and patient selection

We performed a retrospective cohort study at four high-volume gastric cancer treatment centers in three provinces of China. The participating institutions were the Fourth Hospital of Hebei

Medical University, Shijiazhuang People's Hospital, the Fifth Affiliated Hospital of Anhui Medical University in Hefei, and Yichang Central People's Hospital in Hubei. The study protocol was reviewed by the institutional review boards of all four hospitals, with the master ethics approval issued by the Fourth Hospital of Hebei Medical University (reference HEBMU-2024-IRB-031). Because this was a non-interventional analysis of de-identified data already collected for routine clinical care, written informed consent was waived. The study was designed and reported according to the STROBE statement for observational studies.

From the consecutive electronic medical records of 502 patients with gastric or gastroesophageal junction (GEJ) adenocarcinoma seen at the four centers between December 2019 and January 2023, we screened for the following inclusion criteria: histologically confirmed gastric or GEJ adenocarcinoma; clinical stage cT2-4bN_anyM0 by the 8th edition AJCC/UICC TNM system, established by enhanced computed tomography (CT), endoscopic ultrasonography, and 18F-FDG positron emission tomography-CT in selected cases; receipt of at least 2 cycles of neoadjuvant therapy combining a PD-1 inhibitor (camrelizumab, sintilimab, toripalimab, pembrolizumab, or nivolumab) with a platinum-based doublet or triplet chemotherapy regimen (SOX, XELOX, FLOT, or institutional variants); availability of a complete pretreatment laboratory panel measured within 14 days before the start of neoadjuvant therapy, including thyroid function, fasting lipid and glucose values, serum albumin, 25(OH) vitamin D, complete blood count with differential, C-reactive protein, and tumor markers; and subsequent radical gastrectomy with D2 lymphadenectomy and available postoperative pathology, or, in patients who did not undergo surgery, complete records of the reason for omission of surgery.

Patients were excluded if they had radiological or laparoscopic evidence of distant metastasis at any point during pretreatment staging, prior gastrectomy or any prior systemic anticancer therapy for gastric cancer, active autoimmune disease requiring systemic immunosuppression at the time of treatment initiation, severe organ dysfunction precluding chemotherapy, a concurrent active second malignancy, fewer than 2 completed cycles of neoadjuvant therapy, or missing key clinical, pathological, or follow-up data. Of the 502 screened patients, 160 met one or more exclusion criteria and were excluded (Figure 1), leaving a final analytic cohort of 342 patients.

To enable both internal and external assessment of the HNIS prediction model, the analytic cohort was divided into three non-overlapping groups before any model fitting. The training cohort comprised 206 patients drawn from all four participating centers, including all eligible patients from the Fourth Hospital of Hebei Medical University, who served as the model derivation site. The internal validation cohort comprised 68 patients from Shijiazhuang People's Hospital and the Fifth Affiliated Hospital of Anhui Medical University, both of which also contributed patients to the training cohort. The external validation cohort comprised 68 patients from the

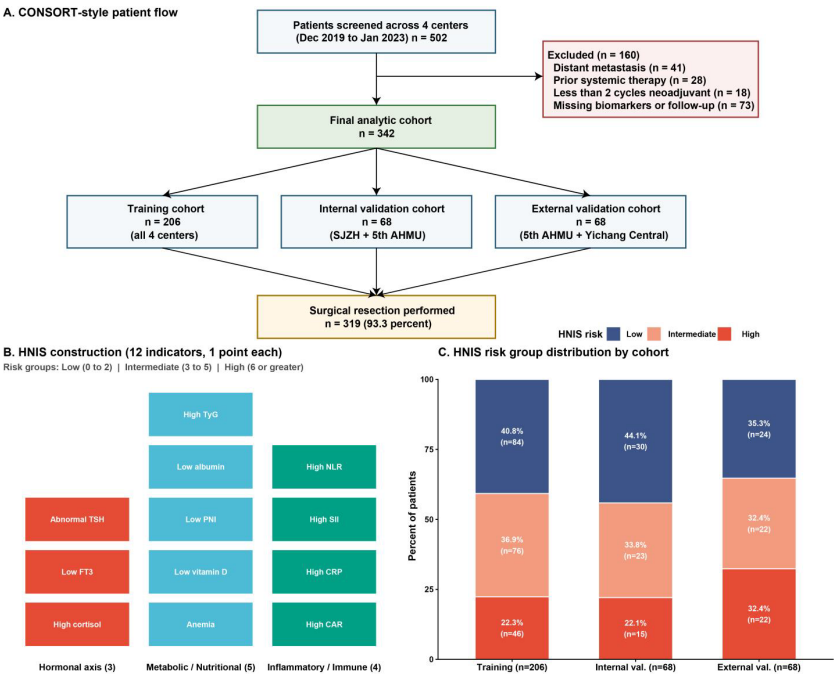

FIGURE 1
Study flow and construction of the Hormonal-Nutritional-Immune Score (HNIS). **(A)** Patient flowchart showing screening of 502 patients, exclusion of 160 patients, inclusion of 342 patients, cohort allocation, and surgical resection status. **(B)** HNIS construction using 12 binary indicators across hormonal (3), metabolic-nutritional (5), and inflammatory-immune (4) domains; one point was assigned for each abnormal indicator. Risk groups were predefined as Low (0–2), Intermediate (3–5), and High (6). **(C)** Distribution of HNIS risk groups in the training, internal validation, and external validation cohorts.

Fifth Affiliated Hospital of Anhui Medical University and Yichang Central People's Hospital, with Yichang Central People's Hospital serving exclusively as an external validation center, providing institutional and geographic separation between the model development and external validation samples. All cohort assignments were made before any biomarker analysis or model construction.

HNIS construction and risk stratification

The Hormonal-Nutritional-Immune Score (HNIS) was a pretreatment, blood-based composite of 12 binary indicators that together covered hormonal axis function, metabolic and nutritional status, and systemic inflammation. One point was assigned for each abnormality, giving a possible total score of 0 to 12. The original score used fixed thresholds drawn from laboratory conventions, previous gastric cancer studies, and study-selected operational definitions. These are not uniformly validated clinical decision thresholds for neoadjuvant immunochemotherapy. Three indicators reflected endocrine status: abnormal thyroid-stimulating hormone (TSH less than 0.55 or greater than 4.78 mIU/L), low free triiodothyronine (FT3 less than 3.1 pmol/L), and high morning serum cortisol (greater than 690 nmol/L). Five indicators reflected metabolic and nutritional status: high triglyceride-glucose (TyG) index defined as TyG greater than 8.8 (calculated as ln[fasting triglycerides (mg/dL) × fasting glucose (mg/dL)/2]), low serum albumin (less than 35 g/L), low prognostic nutritional index (PNI less than 45, calculated as serum albumin (g/L) plus 5 × lymphocyte count (10^9/L)), low 25(OH) vitamin D (less than 20 ng/mL), and anemia (hemoglobin less than 120 g/L in men or less than 110 g/L in women). Four indicators reflected systemic inflammation: high neutrophil-to-lymphocyte ratio (NLR greater than 3), high systemic immune-inflammation index (SII greater than 600, calculated as neutrophil count × platelet count divided by lymphocyte count), high C-reactive protein (CRP greater than 10 mg/L), and high CRP to albumin ratio (CAR greater than 0.30).

The basis and applicability of each cutoff are detailed in Supplementary Table S1. The TSH and FT3 boundaries have assay-based precedents in Chinese studies, but they do not come from a single harmonized assay system (27, 28). The cortisol boundary follows a general morning reference limit (29). Albumin, PNI, hemoglobin, NLR, SII, and CRP have gastric cancer precedents (22, 30–33); the published SII criterion was ≥600 rather than >600, with no boundary-equal values in this dataset. The vitamin D cutoff is a historical definition (34), not an established immunotherapy threshold or a current universal treatment target (35). TyG >8.8 and CAR >0.30 are study-selected operational cutoffs; studies reporting other CAR boundaries support the marker but do not validate 0.30 (26, 36). Center-specific assay reference intervals were not available for this analysis.

The recorded binary indicators were retained for the primary analyses to reproduce the original HNIS. Three records had a displayed albumin concentration of 35.0 g/L and a low-albumin indicator of 1. A sensitivity analysis reapplied the strict <35 g/L rule to the displayed concentrations; the other 11 indicators agreed with their stated cutoffs. No infection-based exclusions or assumptions about correction of nutritional abnormalities were introduced from the laboratory values alone.

For each patient, the HNIS total score was the unweighted sum of the 12 indicators. Patients were then assigned to one of three fixed risk groups: Low risk for a score of 0 to 2, Intermediate risk for a score of 3 to 5, and High risk for a score of 6 or greater. The original 0–2, 3–5, and ≥6 grouping was retained as a descriptive classification, rather than treated as an empirically optimal decision rule. During revision, it was compared with 0–1/2–4/≥5 and 0–3/4–6/≥7 classifications, while the continuous score remained the principal exposure. All added weighting, component-removal, and alternative-classification analyses were exploratory and initiated in response to peer review.

Treatment and follow-up

Patients received at least 2 cycles (typically 3–4 cycles) of neoadjuvant PD-1 inhibitor (camrelizumab, sintilimab, toripalimab, pembrolizumab, or nivolumab) combined with platinum-based chemotherapy: SOX (oxaliplatin 130 mg/m² on day 1 plus S-1 40–60 mg twice daily on days 1–14 of a 21-day cycle), XELOX (oxaliplatin 130 mg/m² on day 1 plus capecitabine 1000 mg/m² twice daily on days 1–14 of a 21-day cycle), FLOT (5-fluorouracil 2600 mg/m², leucovorin 200 mg/m², oxaliplatin 85 mg/m², and docetaxel 50 mg/m²), or institutional variants. Doses and schedules followed institutional protocols and the Chinese Society of Clinical Oncology (CSCO) gastric cancer guidelines. Radiological response was assessed by RECIST v1.1 every 2 cycles. Patients underwent radical gastrectomy with D2 lymphadenectomy 4–6 weeks after the last neoadjuvant cycle. Pathological response was assessed centrally on the resection specimen by two independent board-certified gastrointestinal pathologists at each center using the Mandard tumor regression grading (TRG) system; disagreements were resolved by a third reviewer. Postoperative adjuvant chemotherapy was administered per multidisciplinary tumor-board recommendation.

Patients were followed every 3 months for the first 2 years, every 6 months until 5 years, and annually thereafter. Surveillance included contrast-enhanced CT, tumor markers (CEA, CA19-9), and clinical assessment. Imaging or biopsy was repeated whenever recurrence was clinically suspected. The data cutoff for this analysis was January 31, 2026.

Outcomes and definitions

The primary endpoint was MPR, defined as Mandard TRG 1-2 (≤10% residual viable tumor cells) on the resected specimen. Secondary endpoints were pCR (Mandard TRG 1, no residual viable tumor cells in the primary tumor and any resected lymph nodes), objective response rate (ORR; complete or partial response by RECIST v1.1), disease control rate (DCR; ORR + stable disease), R0 resection, immune-related adverse events (irAEs) graded by CTCAE v5.0 (any-grade and grade ≥3), thyroid-specific irAEs, postoperative complications (Clavien-Dindo grade ≥II), DFS, and OS. DFS was defined as the interval from surgery to disease

recurrence, progression, death from any cause, or last follow-up; for patients who did not undergo surgery, DFS was defined from neoadjuvant therapy initiation. OS was defined as the interval from neoadjuvant therapy initiation to death from any cause or last follow-up. Patients without events were censored at the last follow-up date.

Statistical analysis

Continuous variables were summarized as median and interquartile range (IQR) and compared using the Mann-Whitney U test (two groups) or Kruskal-Wallis test (>2 groups). Categorical variables were summarized as frequency (%) and compared using the χ^2 or Fisher's exact test. Logistic regression was used for binary outcomes (MPR, pCR, ORR, irAEs); variables with $P < 0.10$ in univariable analysis or with established clinical relevance were entered into multivariable models. Survival was estimated by the Kaplan-Meier method, compared by log-rank test, and modeled by univariable and multivariable Cox proportional hazards regression; proportional hazards assumptions were verified by Schoenfeld residuals. The discrimination of HNIS, a clinical staging-based model (age, sex, ECOG PS, cT, cN, PD-L1 CPS, MMR/MSI status, and tumor histology), and the combined HNIS + clinical model was assessed by the area under the receiver operating characteristic curve (AUC) with 95% confidence interval (CI) by DeLong (37), sensitivity, specificity, accuracy, and Brier score (38). Calibration was evaluated by calibration plots and the Hosmer-Lemeshow goodness-of-fit test, and net clinical benefit by decision-curve analysis (39). The training cohort was used for model derivation and the internal validation and external validation cohorts for model assessment without re-fitting. All P values were two-sided, with statistical significance set at $P < 0.05$. Analyses were performed in Python 3.12 (using pandas, scikit-learn, and lifelines) and R 4.3.3 (using the survival, rms, pROC, forestplot, rmda, and ggplot2 packages).

For treatment heterogeneity, we estimated the association per one-point increase in HNIS separately for each PD-1 inhibitor and chemotherapy backbone. Stratum-specific estimates were unadjusted to avoid fitting extensive models within small groups. Pooled adjusted logistic and Cox models included age ≥65 years, sex, ECOG PS ≥1, cT4, cN2–3, PD-L1 CPS ≥5, center, ICI agent, and chemotherapy backbone. For treatment-stratified, pooled adjusted, and risk-group analyses of grade ≥3 irAEs, Firth penalized logistic regression was used because of sparse events; intervals were obtained by profiling the penalized likelihood. Global likelihood-ratio tests compared these models with models adding HNIS-by-agent or HNIS-by-backbone interaction terms. Severe-irAE global tests constrained the interaction or group coefficients to zero within the same full-design Jeffreys-penalized likelihood. Cox models used Breslow handling of tied event times. Secondary endpoint interaction tests were exploratory, particularly for severe irAEs with only 44 events. Nonsignificant interaction tests were not interpreted as demonstrating equivalent effects between regimens.

Each HNIS component was examined separately for MPR, grade ≥3 irAEs, DFS, and OS. Benjamini–Hochberg false-discovery-rate adjustment was applied across the 12 component tests within each endpoint. Component-specific adjusted MPR models added one component at a time to the clinical and treatment covariates listed above. The composite and its constituent variables were not entered together in these added models. Table 1 was also recalculated using separate models for the composite and each listed component, with adjustment for age, sex, and ECOG PS. Pairwise phi correlations and leave-one-component-out comparisons assessed overlap and incremental discrimination.

For MPR, L1-penalized logistic regression used all 12 binary components without preliminary univariable screening. We compared the minimum-loss and one-standard-error penalty rules with the equal-weight score using five-fold stratified outer cross-validation repeated five times. Within each outer training fold, an independent five-fold inner cross-validation selected the penalty

TABLE 1 Univariable and multivariable logistic regression for any-grade immune-related adverse events (irAEs).

Variable	Univariable OR (95% CI)	Univariable P	Multivariable OR (95% CI)	Multivariable P
HNIS total score, per point	1.19 (1.10–1.30)	<0.001	1.15 (1.05–1.27)	0.002
Age ≥ 65 years	1.14 (0.72–1.78)	0.578	0.91 (0.56–1.48)	0.703
Male sex	0.98 (0.62–1.57)	0.945	1.00 (0.61–1.64)	0.990
ECOG PS ≥ 1	2.86 (1.83–4.48)	<0.001	2.42 (1.52–3.86)	<0.001
Abnormal TSH	2.02 (1.12–3.63)	0.019	1.83 (1.00–3.37)	0.051
Low FT3	1.60 (0.87–2.93)	0.131	1.35 (0.72–2.55)	0.349
High cortisol	2.71 (1.59–4.61)	<0.001	2.20 (1.25–3.87)	0.006
Low albumin	1.88 (1.17–3.02)	0.009	1.66 (1.02–2.72)	0.043
Low vitamin D	1.70 (1.09–2.63)	0.018	1.67 (1.06–2.63)	0.027
High NLR	1.36 (0.87–2.13)	0.181	1.26 (0.79–2.02)	0.328
High CRP	1.55 (0.97–2.48)	0.066	1.40 (0.86–2.28)	0.176

HNIS and each listed component were assessed in separate logistic models adjusted for age ≥65 years, male sex, and ECOG PS ≥1. Adjusted estimates for these three clinical covariates are from the model containing the HNIS total. The total score was not entered with its components. Thus, component rows are not coefficients from one mutually adjusted model. Univariable estimates are from separate one-predictor models. Broader clinical- and treatment-adjusted HNIS models are reported in Supplementary Table S3; component analyses for MPR, severe irAEs, DFS, and OS are in Supplementary Table S4. OR, odds ratio; CI, confidence interval.

by log loss from 20 inverse-penalty values C spaced logarithmically from 0.001 to 100. Standardization was fitted within each training fold only. The one-standard-error rule selected the strongest penalty within one standard error of the minimum mean inner-fold loss. All comparisons used the same outer folds. The final illustrative coefficient set was fitted to all 342 patients after performance estimation; its apparent performance was not used as validation.

Cross-validated AUC was calculated from within-test-fold case–control comparisons, weighted by their pair counts over the 25 outer folds, to avoid ranking artifacts from pooling predictions from different fitted models. Brier scores were averaged across the outer test predictions. Paired 95% intervals used 2000 patient-level bootstrap samples, retaining each sampled patient's repeated test predictions. These conditional intervals do not repeat model fitting or penalty selection and therefore do not capture all model-development uncertainty. The added cross-validation analyses are internal validation of the pooled sample and are distinct from the original three-cohort analyses.

Alternative risk-group models used two group indicators and were fitted only in outer training folds. Associations with MPR, severe irAEs, DFS, and OS were also assessed for each classification. Nonlinearity of the continuous HNIS–MPR association was explored with a restricted cubic spline at the 5th, 35th, 65th, and 95th score percentiles (0, 2, 4, and 9). Sensitivity analyses restricted the sample to CRP ≤10 mg/L, albumin ≥35 g/L, no recorded diabetes, or surgery performed, and replaced one component cutoff at a time. These restrictions evaluate dependence on measured baseline abnormalities; they do not define an infection-free or nutritionally corrected cohort. Supplementary Tables S1–S10 give definitions, coefficients, and complete results. The supplemental analyses used NumPy, SciPy, pandas, and scikit-learn; the accompanying scripts record package versions and reproducible random seeds.

Results

Patient characteristics and HNIS distribution

Between December 2019 and January 2023, 342 patients met all inclusion criteria and formed the analytic cohort, distributed across centers as follows: The Fourth Hospital of Hebei Medical University, n=51; Shijiazhuang People's Hospital, n=86; the Fifth Affiliated Hospital of Anhui Medical University, n=120; and Yichang Central People's Hospital, n=85. Patients were assigned to the training cohort (n=206), internal validation cohort (n=68; from Shijiazhuang People's Hospital and the Fifth Affiliated Hospital of Anhui Medical University), and external validation cohort (n=68; from the Fifth Affiliated Hospital of Anhui Medical University and Yichang Central People's Hospital), with the latter providing geographically and institutionally separated validation. The median age was 62 years (IQR 57-67); 233 patients (68.1%) were male and 124 (36.3%) were aged ≥65 years. ECOG performance status was ≥1 in 151 patients (44.2%). The most common tumor location was the lower third of the stomach (38.9%), followed by the middle third (24.9%), upper third (21.1%), and gastroesophageal junction (15.2%). Clinical stage III disease was present in 323 patients (94.4%), and cT4 disease in 140 (40.9%). PD-L1 CPS was ≥5 in 166 patients (48.5%), and dMMR/MSI-H tumors were rare (n=9; 2.6%). Baseline characteristics were generally balanced across the three cohorts (Table 2).

Pretreatment laboratory parameters and HNIS components are summarized in Table 3 and Figure 2A. The median HNIS score was 3 (IQR 2-5) in the overall cohort. Among the 12 individual indicators, the most prevalent abnormalities were low vitamin D (43.6%), high SII (38.9%), high NLR (36.0%), high TyG (36.0%), anemia (35.7%), and low PNI (32.2%). Less common were endocrine-axis abnormalities (abnormal TSH 15.8%, low FT3 14.3%, high cortisol 21.1%). Using the prespecified thresholds, 138 patients (40.4%) were classified as Low risk, 121 (35.4%) as Intermediate risk, and 83 (24.3%) as High risk. The HNIS distribution did not differ significantly across cohorts (P = 0.222), although the external validation cohort had a non-significantly higher proportion of High-risk patients (35.3% vs. 22.3% in training).

Treatment exposure, pathological response, and immune-related toxicity

Treatment-related characteristics and outcomes are detailed in Table 4. Sintilimab was the most commonly used PD-1 inhibitor (37.7%), followed by camrelizumab (32.7%) and toripalimab (19.3%); pembrolizumab and nivolumab were used in 5.3% and 5.0% of patients, respectively. Chemotherapy backbones were SOX in 50.6%, FLOT in 14.6%, XELOX in 12.6%, and other regimens in 22.2%. Most patients (91.2%) completed at least 3 neoadjuvant cycles. Radical gastrectomy was performed in 319 patients (93.3%), with R0 resection achieved in 279 (81.6% of all patients, 87.5% of those operated). Across the cohort, pCR was observed in 40 patients (11.7%), MPR in 166 (48.5%), ORR in 193 (56.4%), and DCR in 325 (95.0%). Any-grade irAEs occurred in 134 patients (39.2%), grade ≥3 irAEs in 44 (12.9%), thyroid irAEs in 30 (8.8%), and other endocrine irAEs in 44 (12.9%). Postoperative Clavien-Dindo grade ≥II complications occurred in 105 patients (30.7%). The median follow-up was 52.5 months (IQR 41.5-65.3), during which 202 DFS events (59.1%) and 77 OS events (22.5%) were recorded.

Association between HNIS and pathological response

A clear monotonic gradient in pathological response was observed across HNIS risk groups (Table 5; Figure 2B). MPR rates declined from 67.4% in the Low-risk group to 46.3% in the Intermediate-risk group and 20.5% in the High-risk group (P<0.001), and pCR rates from 20.3% to 7.4% to 3.6% (P<0.001). ORR was also significantly different across groups (65.9% vs. 52.1% vs. 47.0%, P = 0.011), and the rate of R0 resection declined from 86.2% to 82.6% to 72.3% (P = 0.033). In multivariable logistic regression for MPR, adjusted for age, ECOG PS, cT4 disease, cN2–3 disease, PD-L1 CPS ≥5, MMR status, Lauren type, differentiation, and baseline tumor markers, each one-point increase in HNIS was independently associated with lower odds of MPR (adjusted OR

10.3389/fimmu.2026.1875198

TABLE 2 Baseline clinical and tumor characteristics of the analytic cohort by training, internal validation, and external validation cohort.

Variable	Overall (n=342)	Training (n=206)	Internal validation (n=68)	External validation (n=68)	P value
Age, years	62 (57-67)	62 (57-67)	62 (56-68)	63 (57-68)	0.661
Age ≥ 65 years	124 (36.3)	72 (35.0)	24 (35.3)	28 (41.2)	0.640
Male sex	233 (68.1)	141 (68.4)	44 (64.7)	48 (70.6)	0.754
BMI, kg/m²	22.8 (21.2-24.4)	22.9 (21.1-24.4)	22.9 (21.6-25.1)	22.8 (21.2-24.2)	0.670
ECOG PS ≥ 1	151 (44.2)	88 (42.7)	28 (41.2)	35 (51.5)	0.388
Smoking status					0.792
Never	112 (32.7)	71 (34.5)	20 (29.4)	21 (30.9)	
Former	114 (33.3)	70 (34.0)	21 (30.9)	23 (33.8)	
Current	116 (33.9)	65 (31.6)	27 (39.7)	24 (35.3)	
Alcohol history	118 (34.5)	71 (34.5)	28 (41.2)	19 (27.9)	0.268
Diabetes	54 (15.8)	41 (19.9)	8 (11.8)	5 (7.4)	0.029
Hypertension	115 (33.6)	65 (31.6)	25 (36.8)	25 (36.8)	0.608
Tumor location					0.813
Lower third	133 (38.9)	80 (38.8)	26 (38.2)	27 (39.7)	
Middle third	85 (24.9)	50 (24.3)	19 (27.9)	16 (23.5)	
Upper third	72 (21.1)	40 (19.4)	16 (23.5)	16 (23.5)	
GEJ	52 (15.2)	36 (17.5)	7 (10.3)	9 (13.2)	
Clinical T stage					0.551
cT2	35 (10.2)	22 (10.7)	3 (4.4)	10 (14.7)	
cT3	167 (48.8)	100 (48.5)	34 (50.0)	33 (48.5)	
cT4a	106 (31.0)	63 (30.6)	25 (36.8)	18 (26.5)	
cT4b	34 (9.9)	21 (10.2)	6 (8.8)	7 (10.3)	
cT4 disease	140 (40.9)	84 (40.8)	31 (45.6)	25 (36.8)	0.577
Clinical N stage					0.403
cN0	61 (17.8)	34 (16.5)	15 (22.1)	12 (17.6)	
cN1	98 (28.7)	66 (32.0)	18 (26.5)	14 (20.6)	
cN2	112 (32.7)	68 (33.0)	18 (26.5)	26 (38.2)	
cN3	71 (20.8)	38 (18.4)	17 (25.0)	16 (23.5)	
cN2–3 disease	183 (53.5)	106 (51.5)	35 (51.5)	42 (61.8)	0.313
Clinical stage III	323 (94.4)	192 (93.2)	66 (97.1)	65 (95.6)	0.436
Lauren type					0.703
Intestinal	135 (39.5)	80 (38.8)	30 (44.1)	25 (36.8)	
Diffuse	124 (36.3)	73 (35.4)	26 (38.2)	25 (36.8)	
Mixed	83 (24.3)	53 (25.7)	12 (17.6)	18 (26.5)	
Poor/undifferentiated	251 (73.4)	143 (69.4)	52 (76.5)	56 (82.4)	0.091
HER2 positive	42 (12.3)	23 (11.2)	9 (13.2)	10 (14.7)	0.716
PD-L1 CPS	4.8 (2.7-9.5)	4.8 (2.7-9.7)	4.2 (2.2-7.2)	5.5 (3.1-10.7)	0.222
PD-L1 CPS ≥ 5	166 (48.5)	101 (49.0)	30 (44.1)	35 (51.5)	0.675
dMMR/MSI-H	9 (2.6)	3 (1.5)	4 (5.9)	2 (2.9)	0.139
CEA, ng/mL	3.7 (2.2-6.0)	3.6 (2.1-6.1)	4.5 (2.6-6.7)	3.3 (2.4-5.0)	0.139
CA19-9, U/mL	20.0 (11.5-40.8)	18.3 (10.4-37.8)	30.7 (13.9-47.6)	19.6 (11.4-39.8)	0.039

Continuous variables are presented as median (interquartile range) and were compared using the Kruskal-Wallis test. Categorical variables are presented as n (%) and were compared using the χ^2 test or Fisher's exact test as appropriate. ECOG PS, Eastern Cooperative Oncology Group performance status; BMI, body mass index; GEJ, gastroesophageal junction; CPS, combined positive score; PD-L1, programmed cell death ligand 1; dMMR, deficient mismatch repair; MSI-H, microsatellite-instability high; CEA, carcinoembryonic antigen; CA19-9, carbohydrate antigen 19-9.

10.3389/fimmu.2026.1875198

TABLE 3 Baseline hormonal, metabolic, nutritional, and inflammatory biomarkers and the Hormonal-Nutritional-Immune Score (HNIS) by cohort.

Variable	Overall (n=342)	Training (n=206)	Internal validation (n=68)	External validation (n=68)	P value
TSH, mIU/L	2.8 (1.7-4.1)	2.7 (1.7-3.7)	3.1 (1.8-4.1)	2.9 (1.7-4.3)	0.174
FT3, pmol/L	4.5 (4.0-4.8)	4.5 (4.0-4.9)	4.4 (4.1-4.8)	4.4 (3.6-4.8)	0.353
FT4, pmol/L	14.9 (13.8-15.9)	15.0 (13.7-15.9)	14.7 (13.7-15.8)	14.8 (13.9-15.8)	0.649
Abnormal TSH	54 (15.8)	28 (13.6)	10 (14.7)	16 (23.5)	0.144
Low FT3	49 (14.3)	26 (12.6)	8 (11.8)	15 (22.1)	0.125
Morning cortisol, nmol/L	441.5 (377.0-561.8)	446.5 (378.2-560.8)	440.5 (376.8-509.8)	439.0 (371.8-761.8)	0.852
High cortisol	72 (21.1)	42 (20.4)	12 (17.6)	18 (26.5)	0.421
Triglycerides, mmol/L	1.3 (1.0-2.2)	1.3 (1.0-2.2)	1.3 (1.1-2.0)	1.3 (1.0-2.4)	0.830
Fasting glucose, mmol/L	5.5 (5.2-5.9)	5.5 (5.2-6.0)	5.6 (5.3-5.8)	5.4 (5.1-5.7)	0.190
TyG index	8.7 (8.4-9.2)	8.7 (8.4-9.2)	8.7 (8.5-9.0)	8.6 (8.3-9.3)	0.629
High TyG (>8.8)	123 (36.0)	73 (35.4)	23 (33.8)	27 (39.7)	0.751
Albumin, g/L	38.4 (33.5-40.2)	38.3 (34.1-40.4)	38.5 (34.3-40.2)	38.3 (33.1-40.1)	0.624
Prealbumin, mg/L	191.0 (139.8-225.8)	191.5 (139.0-223.8)	186.5 (136.5-224.0)	196.0 (151.8-230.0)	0.925
PNI	47.4 (42.6-51.3)	47.4 (42.4-51.3)	46.7 (43.0-51.7)	47.5 (43.5-51.3)	0.993
Low albumin (<35 g/L)	100 (29.2)	58 (28.2)	19 (27.9)	23 (33.8)	0.650
Low PNI (<45)	110 (32.2)	67 (32.5)	24 (35.3)	19 (27.9)	0.646
25(OH)Vitamin D, ng/mL	23.3 (12.2-33.1)	23.0 (11.9-33.1)	24.1 (12.3-33.2)	25.1 (14.8-32.0)	0.965
Low vitamin D (<20 ng/mL)	149 (43.6)	90 (43.7)	30 (44.1)	29 (42.6)	0.984
Hemoglobin, g/L	124.0 (101.0-134.0)	124.0 (101.2-135.0)	124.0 (107.8-134.0)	120.0 (92.8-134.0)	0.269
Anemia	122 (35.7)	72 (35.0)	20 (29.4)	30 (44.1)	0.190
Ferritin, ng/mL	148.8 (102.5-227.0)	145.3 (99.5-222.0)	162.1 (112.2-239.6)	143.0 (102.8-228.6)	0.341
Transferrin, g/L	2.3 (2.1-2.5)	2.3 (2.1-2.5)	2.3 (2.1-2.6)	2.2 (2.1-2.5)	0.294
NLR	2.3 (1.5-4.8)	2.3 (1.5-4.4)	2.2 (1.6-5.2)	2.4 (1.5-4.8)	0.782
SII	508.1 (332.8-914.8)	503.3 (335.9-899.8)	519.6 (324.4-910.8)	507.7 (338.5-1002.3)	0.865
CRP, mg/L	7.2 (3.9-19.0)	6.6 (3.4-13.5)	7.2 (4.6-9.7)	9.0 (5.0-36.1)	0.016
CAR (CRP/Albumin)	0.2 (0.1-0.6)	0.2 (0.1-0.4)	0.2 (0.1-0.3)	0.2 (0.1-0.9)	0.015
High NLR (>3)	123 (36.0)	74 (35.9)	23 (33.8)	26 (38.2)	0.866
High SII (>600)	133 (38.9)	79 (38.3)	26 (38.2)	28 (41.2)	0.911
High CRP (>10 mg/L)	103 (30.1)	57 (27.7)	16 (23.5)	30 (44.1)	0.016
High CAR (>0.3)	104 (30.4)	59 (28.6)	15 (22.1)	30 (44.1)	0.014
HNIS total score	3.0 (2.0-5.0)	3.0 (2.0-5.0)	3.0 (2.0-5.0)	4.0 (1.8-6.2)	0.222
HNIS risk group					0.204
Low	138 (40.4)	86 (41.7)	29 (42.6)	23 (33.8)	
Intermediate	121 (35.4)	74 (35.9)	26 (38.2)	21 (30.9)	
High	83 (24.3)	46 (22.3)	13 (19.1)	24 (35.3)	

Values are median (interquartile range) for continuous variables and n (%) for categorical variables. The HNIS score sums 12 binary abnormalities (1 point each) across hormonal (abnormal TSH, low FT3, high cortisol), metabolic-nutritional (high TyG, low albumin, low PNI, low vitamin D, anemia), and inflammatory (high NLR, high SII, high CRP, high CAR) axes; risk groups were prespecified as Low (0-2), Intermediate (3-5), and High (≥6). TSH, thyroid-stimulating hormone; FT3, free triiodothyronine; FT4, free thyroxine; TyG, triglyceride-glucose index; PNI, prognostic nutritional index; NLR, neutrophil-to-lymphocyte ratio; SII, systemic immune-inflammation index; CRP, C-reactive protein; CAR, CRP/albumin ratio.

0.68, 95% CI 0.61-0.76; P<0.001) (Table 6). Risk-group analysis confirmed a graded effect: compared with Low-risk patients, Intermediate-risk patients had adjusted OR 0.42 (95% CI 0.25-0.70; P = 0.001) and High-risk patients had adjusted OR 0.13 (95% CI 0.06-0.25; P<0.001) for MPR.

HNIS and immune-related adverse events

Higher HNIS was associated with an increased risk of irAEs (Table 5). Any-grade irAEs occurred in 31.2% of Low-risk, 39.7% of Intermediate-risk, and 51.8% of High-risk patients (P = 0.010), and

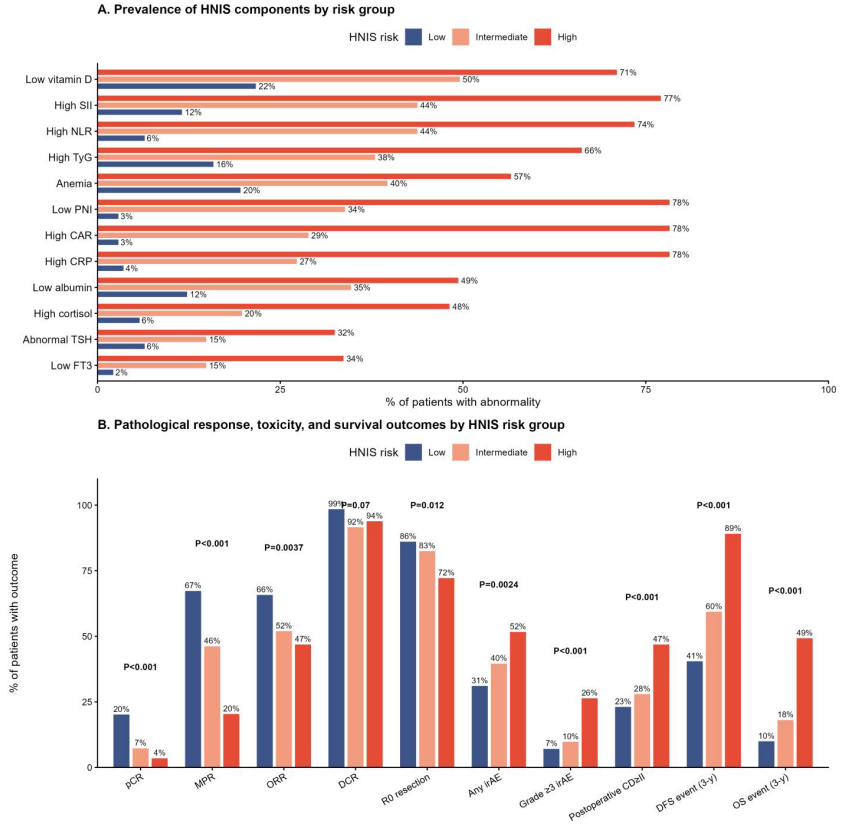

FIGURE 2
Distribution of HNIS components and clinical outcomes by HNIS risk group. **(A)** Bar plots showing the prevalence of each of the 12 HNIS abnormalities across the Low-, Intermediate-, and High-risk groups. **(B)** Bar plots of pathological response (pCR, MPR, ORR), surgical outcome (R0 resection), immune-related toxicity (any-grade irAEs, grade 3 or higher irAEs), postoperative complications (Clavien-Dindo grade II or higher), and survival events (3-year DFS event, 3-year OS event) across HNIS risk groups, with significance of the linear trend across groups indicated above each set of bars (Cochran-Armitage trend test, all P<0.05).

grade 3 or higher irAEs occurred in 7.2%, 9.9%, and 26.5%, respectively (P<0.001). Univariable logistic regression confirmed that each one-point HNIS increase was associated with higher odds of any-grade irAEs (OR 1.19, 95% CI 1.10 to 1.30; P<0.001) and a marked rise for grade 3 or higher events (OR 1.30 per point, 95% CI 1.16 to 1.47; P<0.001). To avoid overlap between the total score and its components, we fitted separate models adjusted for age, sex, and ECOG PS. HNIS remained associated with any-grade irAEs (adjusted OR 1.15 (1.05–1.27); P = 0.002) (Table 1). Component-specific estimates describe separate adjusted associations and do not establish mutually independent effects. With additional adjustment for clinical stage, PD-L1 CPS, center, ICI agent, and chemotherapy backbone, the OR per HNIS point was 1.16 (1.05–1.28) for any-grade irAEs and 1.27 (1.12–1.45) for grade ≥3 irAEs (Supplementary Table S3).

Survival analysis

Kaplan-Meier estimates of disease-free and overall survival by HNIS risk group are shown in Figure 3 and Table 5. The 1-, 2-, and 3-year DFS rates were 86.2%, 75.4%, and 69.6% in the Low-risk group; 82.6%, 67.8%, and 58.7% in the Intermediate-risk group; and 57.8%, 32.5%, and 24.1% in the High-risk group (log-rank P<0.001). The corresponding 1-, 2-, and 3-year OS rates were 97.8%, 95.7%, and 94.9% in Low-risk; 96.7%, 92.6%, and 87.6% in Intermediate-risk; and 89.2%, 84.3%, and 69.9% in High-risk (log-rank P<0.001). DFS event rates by group were 40.6%, 59.5%, and 89.2% (P<0.001), and OS event rates were 10.1%, 18.2%, and 49.4% (P<0.001) (Table 5).

In multivariable Cox regression adjusting for age, sex, ECOG PS, cT4 disease, cN2–3 disease, PD-L1 CPS ≥5, MMR/MSI status, pCR, and tumor histology, each one-point increase in HNIS was independently associated with worse DFS (adjusted HR 1.25, 95% CI 1.18-1.33; P<0.001) and worse OS (adjusted HR 1.34, 95% CI 1.21-1.47; P<0.001) (Table 7). Age ≥65 years (DFS HR 1.86, 95% CI 1.39-2.48; OS HR 2.22, 95% CI 1.37-3.58), cT4 disease (OS HR 1.85, 95% CI 1.16-2.94), cN2–3 disease (OS HR 1.87, 95% CI 1.14-3.06), and pCR (DFS HR 0.15, 95% CI 0.06-0.42) were also independent predictors. Schoenfeld residual testing did not detect violations of the proportional hazards assumption for HNIS (global P = 0.31).

Predictive performance for major pathological response

Across all three cohorts, HNIS substantially outperformed a clinical model based on standard staging and tumor biomarkers for prediction of MPR (Table 8; Figure 4). In the training cohort, AUCs were 0.611 (95% CI 0.530-0.684) for the clinical model, 0.725

TABLE 4 Treatment exposure, pathological and radiological response, safety, and follow-up outcomes by cohort.

Variable	Overall (n=342)	Training (n=206)	Internal validation (n=68)	External validation (n=68)	P value
ICI agent					0.400
Pembrolizumab	18 (5.3)	12 (5.8)	2 (2.9)	4 (5.9)	
Nivolumab	17 (5.0)	10 (4.9)	4 (5.9)	3 (4.4)	
Sintilimab	129 (37.7)	83 (40.3)	28 (41.2)	18 (26.5)	
Toripalimab	66 (19.3)	41 (19.9)	13 (19.1)	12 (17.6)	
Camrelizumab	112 (32.7)	60 (29.1)	21 (30.9)	31 (45.6)	
Chemotherapy backbone					0.069
SOX	173 (50.6)	98 (47.6)	35 (51.5)	40 (58.8)	
FLOT	50 (14.6)	29 (14.1)	8 (11.8)	13 (19.1)	
XELOX	43 (12.6)	28 (13.6)	13 (19.1)	2 (2.9)	
Other	76 (22.2)	51 (24.8)	12 (17.6)	13 (19.1)	
≥ 3 neoadjuvant cycles	312 (91.2)	182 (88.3)	64 (94.1)	66 (97.1)	0.057
Surgery performed	319 (93.3)	190 (92.2)	62 (91.2)	67 (98.5)	0.148
Surgical approach (operated)					0.912
Open	106 (31.0)	67 (32.5)	18 (26.5)	21 (30.9)	
Laparoscopic	173 (50.6)	100 (48.5)	36 (52.9)	37 (54.4)	
Robotic	40 (11.7)	23 (11.2)	8 (11.8)	9 (13.2)	
R0 resection	279 (81.6)	172 (83.5)	55 (80.9)	52 (76.5)	0.426
pCR	40 (11.7)	21 (10.2)	8 (11.8)	11 (16.2)	0.412
MPR	166 (48.5)	102 (49.5)	34 (50.0)	30 (44.1)	0.716
ORR	193 (56.4)	117 (56.8)	34 (50.0)	42 (61.8)	0.379
DCR	325 (95.0)	195 (94.7)	64 (94.1)	66 (97.1)	0.680
Any irAE	134 (39.2)	80 (38.8)	21 (30.9)	33 (48.5)	0.107
Grade ≥3 irAE	44 (12.9)	23 (11.2)	9 (13.2)	12 (17.6)	0.382
Thyroid irAE	30 (8.8)	18 (8.7)	5 (7.4)	7 (10.3)	0.832
Endocrine irAE	44 (12.9)	25 (12.1)	6 (8.8)	13 (19.1)	0.177
Postoperative CD≥II complication	105 (30.7)	63 (30.6)	21 (30.9)	21 (30.9)	0.998
Follow-up, months	52.5 (41.5-65.3)	51.6 (41.2-63.5)	52.4 (41.1-68.3)	54.2 (43.8-65.0)	0.679
DFS event	202 (59.1)	122 (59.2)	39 (57.4)	41 (60.3)	0.938
OS event	77 (22.5)	42 (20.4)	15 (22.1)	20 (29.4)	0.302

Values are n (%) unless indicated. Pathological complete response (pCR) is Mandard tumor regression grade (TRG) 1; major pathological response (MPR) is TRG 1-2 (≤10% residual viable tumor cells). Objective response rate (ORR) is partial or complete radiographic response by RECIST v1.1; disease control rate (DCR) is ORR plus stable disease. Immune-related adverse events (irAEs) were graded according to CTCAE v5.0. Postoperative complications were graded according to the Clavien-Dindo classification. SOX, S-1 + oxaliplatin; XELOX, capecitabine + oxaliplatin; FLOT, 5-fluorouracil + leucovorin + oxaliplatin + docetaxel; DFS, disease-free survival; OS, overall survival.

(0.655-0.788) for HNIS, and 0.745 (0.673-0.805) for the combined HNIS + clinical model. In the internal validation cohort, AUCs were 0.569, 0.736, and 0.729, and in the external validation cohort, 0.554, 0.753, and 0.719, respectively. DeLong tests indicated that HNIS-based models had significantly higher AUC than the clinical model in all three cohorts (all P<0.05), whereas the addition of clinical features to HNIS did not significantly improve discrimination beyond HNIS alone (DeLong P = 0.21-0.74). Brier scores were lower for the HNIS and combined models (0.200-0.214) than for the clinical model (0.242-0.249) across cohorts, indicating better calibration. At the prespecified probability threshold of 0.534, HNIS achieved a sensitivity of 60.0-76.5% and a specificity of 63.5-71.1% across cohorts. Decision-curve analysis demonstrated higher net clinical benefit for the HNIS-based models across threshold probabilities of approximately 0.10-0.65.

Subgroup and sensitivity analyses

Treatment-stratified MPR odds ratios per HNIS point ranged from 0.62 to 0.87 across the five PD-1 inhibitors and from 0.59 to 0.73 across chemotherapy backbones (Supplementary Table S2). After adjustment for clinical factors, center, ICI agent, and chemotherapy backbone, the MPR OR was 0.68 (95% CI 0.61–0.76). Global interaction P values for ICI agent and chemotherapy backbone were 0.348 and 0.521 for MPR, 0.680 and 0.626 for grade ≥3 irAEs, 0.886 and 0.187 for DFS, and 0.264 and 0.147 for

TABLE 5 Pathological response, immune-related toxicity, postoperative complications, and survival outcomes by HNIS risk group.

Outcome	Overall (n=342)	Low risk (n=138)	Intermediate (n=121)	High risk (n=83)	P value
pCR	40 (11.7)	28 (20.3)	9 (7.4)	3 (3.6)	<0.001
MPR	166 (48.5)	93 (67.4)	56 (46.3)	17 (20.5)	<0.001
ORR	193 (56.4)	91 (65.9)	63 (52.1)	39 (47.0)	0.011
DCR	325 (95.0)	136 (98.6)	111 (91.7)	78 (94.0)	0.037
R0 resection	279 (81.6)	119 (86.2)	100 (82.6)	60 (72.3)	0.033
Any irAE	134 (39.2)	43 (31.2)	48 (39.7)	43 (51.8)	0.010
Grade ≥3 irAE	44 (12.9)	10 (7.2)	12 (9.9)	22 (26.5)	<0.001
Thyroid irAE	30 (8.8)	6 (4.3)	15 (12.4)	9 (10.8)	0.055
Postoperative CD≥II complication	105 (30.7)	32 (23.2)	34 (28.1)	39 (47.0)	<0.001
DFS event	202 (59.1)	56 (40.6)	72 (59.5)	74 (89.2)	<0.001
OS event	77 (22.5)	14 (10.1)	22 (18.2)	41 (49.4)	<0.001
Follow-up, months	52.5 (41.5-65.3)	55.8 (45.9-69.0)	52.1 (42.4-64.7)	47.0 (29.2-58.6)	<0.001
DFS time, months	39.1 (14.0-53.4)	47.1 (26.1-62.9)	42.3 (17.4-53.2)	15.2 (6.2-35.2)	<0.001
OS time, months	52.5 (41.5-65.3)	55.8 (45.9-69.0)	52.1 (42.4-64.7)	47.0 (29.2-58.6)	<0.001

Values are n (%) unless indicated. P values are for the test of trend across HNIS groups (Cochran-Armitage for binary outcomes, Kruskal-Wallis for continuous variables). DFS event refers to disease recurrence, progression, or death from any cause within the follow-up period; OS event refers to death from any cause.

OS, respectively (Supplementary Table S3). The pembrolizumab (n=18) and nivolumab (n=17) strata had wide confidence intervals. These results show no detected heterogeneity, but do not establish regimen equivalence or exclude clinically relevant differences in small strata.

All 12 binary components were associated with MPR, DFS, and OS after endpoint-specific false-discovery-rate adjustment in univariable analyses; three were associated with grade ≥3 irAEs (Supplementary Table S4). Eleven components retained an adjusted MPR association after correction, whereas high cortisol did not (adjusted OR 0.59, 95% CI 0.33–1.07; P = 0.083). Correlation was particularly strong between high CRP and high CAR (phi=0.965), showing that component count does not equal the number of independent biological signals (Supplementary Table S10).

The one-standard-error LASSO fit retained nine components and set the coefficients for high cortisol, low vitamin D, and high CRP to zero. Their selection frequencies in the 25 outer training fits were 8%, 36%, and 4%, respectively (Supplementary Table S5). Cross-validated AUCs were 0.733 (0.681–0.784) for the equal-weight score, 0.708 (0.654–0.760) for minimum-loss LASSO, and 0.704 (0.651–0.756) for one-standard-error LASSO; corresponding Brier scores were 0.208, 0.217, and 0.220 (Supplementary Table S6). The weighted models did not improve discrimination in this internal comparison. Omitting cortisol, vitamin D, or CRP

TABLE 6 Univariable and multivariable logistic regression for major pathological response (MPR).

Variable	Univariable OR (95% CI)	Univariable P	Multivariable OR (95% CI)	Multivariable P
HNIS total score, per point	0.69 (0.62-0.76)	<0.001	0.68 (0.61-0.76)	<0.001
HNIS Intermediate vs. Low	0.50 (0.30-0.84)	0.008	0.42 (0.25-0.70)	0.001
HNIS High vs. Low	0.13 (0.06-0.25)	<0.001	0.13 (0.06-0.25)	<0.001
Age ≥ 65 years	0.85 (0.55-1.32)	0.473	1.16 (0.70-1.94)	0.560
Male sex	1.05 (0.67-1.66)	0.833	NA	NA
ECOG PS ≥ 1	0.58 (0.38-0.90)	0.014	0.83 (0.51-1.36)	0.470
cT4 disease	1.22 (0.79-1.87)	0.373	1.17 (0.72-1.92)	0.519
cN2–3 disease	0.80 (0.52-1.22)	0.296	0.84 (0.52-1.38)	0.498
PD-L1 CPS ≥ 5	1.49 (0.97-2.28)	0.069	1.48 (0.92-2.38)	0.110
dMMR/MSI-H	3.83 (0.78-18.71)	0.097	2.46 (0.45-13.44)	0.299
Lauren intestinal type	1.37 (0.89-2.12)	0.152	1.31 (0.77-2.23)	0.327
Poor/undifferentiated histology	0.75 (0.46-1.21)	0.238	0.76 (0.41-1.41)	0.383
CEA > 5 ng/mL	0.82 (0.53-1.29)	0.393	0.78 (0.47-1.30)	0.342
CA19-9 > 37 U/mL	1.08 (0.68-1.74)	0.735	1.52 (0.88-2.62)	0.133

Multivariable model included all variables with P<0.10 in univariable analysis or established clinical relevance. OR, odds ratio; CI, confidence interval. NA indicates that the variable was not entered into the multivariable model due to collinearity or because it is the primary exposure of interest.

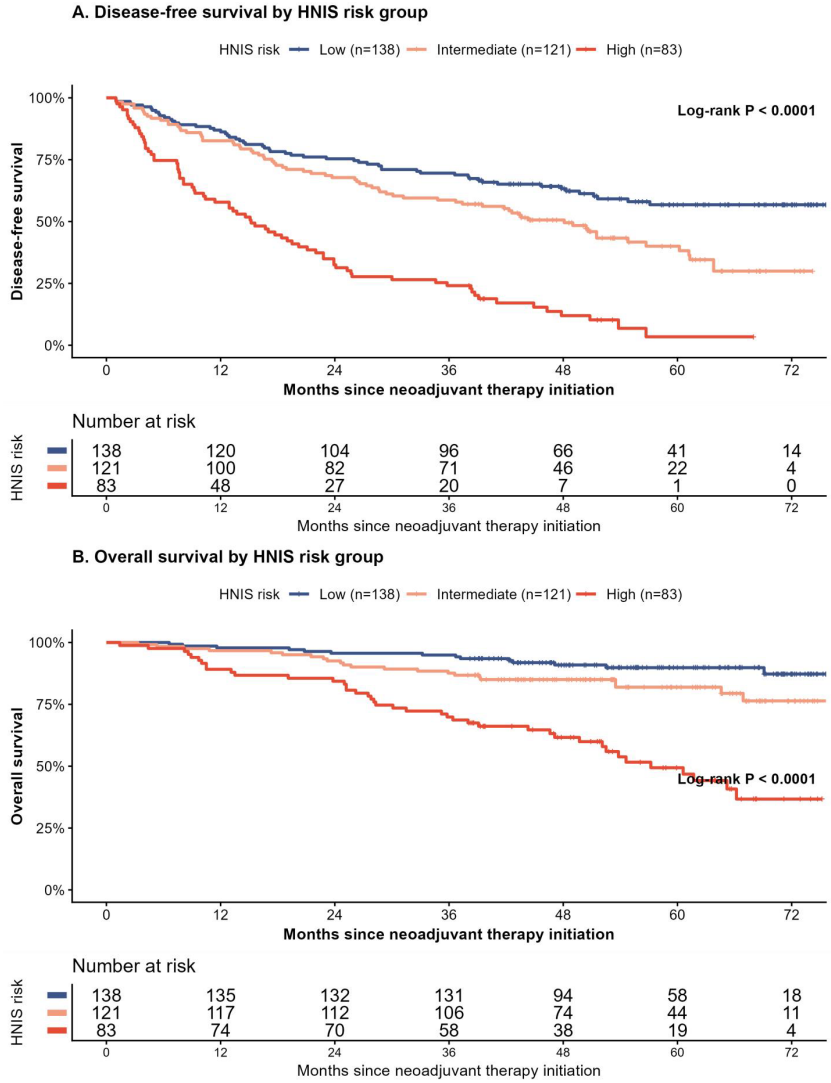

FIGURE 3
Kaplan-Meier survival curves stratified by HNIS risk group. **(A)** Disease-free survival; 1-, 2-, and 3-year DFS rates were 86.2%, 75.4%, and 69.6% in Low-risk; 82.6%, 67.8%, and 58.7% in Intermediate-risk; and 57.8%, 32.5%, and 24.1% in High-risk patients (log-rank P<0.001). **(B)** Overall survival; 1-, 2-, and 3-year OS rates were 97.8%, 95.7%, and 94.9% in Low-risk; 96.7%, 92.6%, and 87.6% in Intermediate-risk; and 89.2%, 84.3%, and 69.9% in High-risk patients (log-rank P<0.001). Numbers at risk are displayed below each panel. Censored events are indicated by tick marks on the survival curves.

individually changed AUC by only +0.0005, +0.003, and +0.003, respectively, with conditional 95% intervals crossing zero. These findings indicate limited incremental MPR information from some components, rather than proving that every component is necessary or that a zero coefficient implies biological irrelevance.

The original, 0–1/2–4/≥5, and 0–3/4–6/≥7 classifications yielded cross-validated MPR AUCs of 0.696, 0.697, and 0.711, respectively, compared with 0.733 for continuous HNIS (Supplementary Tables S6, S7). MPR rates across the alternative classifications were 69.0%/56.8%/22.3% and 66.7%/35.9%/15.3%, respectively. Both alternatives also separated toxicity and survival outcomes. The spline analysis did not detect nonlinearity (P = 0.758). Thus, the original boundaries are useful descriptive strata but were not demonstrated to be the optimal classification.

In sensitivity analyses, the adjusted MPR OR per HNIS point was 0.68 (95% CI 0.58–0.80) among patients with CRP ≤10 mg/L (n=239), 0.74 (0.64–0.84) among those with albumin ≥35 g/L (n=239), 0.72 (0.64–0.81) among those without recorded diabetes (n=288), and 0.66 (0.59–0.74) among operated patients (n=319) (Supplementary Table S8). Replacing one component threshold at a time yielded ORs between 0.66 and 0.69; however, the alternative CAR cutoff changed risk-group assignment in 56 patients, indicating that similar overall associations do not imply interchangeable patient-level classification (Supplementary Table S9). Strict recoding of the three albumin boundary records changed no risk groups and gave an adjusted OR of 0.68 (95% CI 0.61–0.76).

Discussion

In this multicenter retrospective cohort of 342 patients with locally advanced gastric or GEJ adenocarcinoma treated with neoadjuvant PD-1 inhibitor plus platinum-based chemotherapy, a

TABLE 7 Univariable and multivariable Cox proportional hazards regression for disease-free survival (DFS) and overall survival (OS).

Variable	DFS Univariable HR (95% CI)	DFS Univ. P	DFS Multivariable HR (95% CI)	DFS Multiv. P	OS Univariable HR (95% CI)	OS Univ. P	OS Multivariable HR (95% CI)	OS Multiv. P
HNIS total score, per point	1.29 (1.22-1.37)	<0.001	1.25 (1.18-1.33)	<0.001	1.42 (1.30-1.55)	<0.001	1.34 (1.21-1.47)	<0.001
Age ≥ 65 years	1.99 (1.51-2.63)	<0.001	1.86 (1.39-2.48)	<0.001	2.89 (1.83-4.54)	<0.001	2.22 (1.37-3.58)	0.001
Male sex	0.96 (0.72-1.30)	0.811	0.87 (0.64-1.18)	0.367	0.93 (0.58-1.49)	0.761	0.83 (0.51-1.34)	0.435
ECOG PS ≥ 1	1.31 (0.99-1.72)	0.056	0.89 (0.67-1.20)	0.450	1.63 (1.04-2.55)	0.033	1.10 (0.69-1.76)	0.688
cT4 disease	1.22 (0.93-1.61)	0.155	1.33 (1.00-1.77)	0.050	1.43 (0.92-2.24)	0.116	1.85 (1.16-2.94)	0.009
cN2–3 disease	1.00 (0.76-1.32)	0.982	1.02 (0.77-1.35)	0.889	1.80 (1.12-2.89)	0.014	1.87 (1.14-3.06)	0.013
PD-L1 CPS ≥ 5	0.74 (0.56-0.98)	0.037	0.87 (0.65-1.15)	0.321	0.67 (0.43-1.06)	0.089	0.77 (0.48-1.24)	0.283
dMMR/MSI-H	0.13 (0.02-0.91)	0.040	0.16 (0.02-1.14)	0.068	0.00 (0.00-inf)	0.996	0.00 (0.00-inf)	0.998
pCR	0.10 (0.04-0.27)	<0.001	0.15 (0.06-0.42)	<0.001	0.00 (0.00-inf)	0.994	0.00 (0.00-inf)	0.995
MPR	0.53 (0.40-0.70)	<0.001	NA	NA	0.28 (0.16-0.47)	<0.001	NA	NA
Poor/undifferentiated histology	0.93 (0.68-1.27)	0.665	0.93 (0.68-1.27)	0.642	0.83 (0.51-1.36)	0.468	1.19 (0.71-1.97)	0.510

Multivariable Cox regression included variables with P<0.10 in univariable analysis or established clinical relevance: HNIS (continuous, per one-point increment), age 65 years or older, male sex, ECOG PS 1 or higher, cT4 disease, cN2 to cN3 disease, PD-L1 CPS 5 or higher, dMMR or MSI-H status, pCR status, and tumor histology. Schoenfeld residual testing did not detect violations of the proportional hazards assumption for HNIS (global P = 0.31). HR, hazard ratio; CI, confidence interval. The very small number of OS events among dMMR or MSI-H and pCR-attaining patients precluded stable coefficient estimation for those covariates in the OS multivariable model and is shown as an empty entry; the corresponding univariable estimates remain valid. NA indicates that the variable was not entered into the multivariable model.

10.3389/fimmu.2026.1875198

TABLE 8 **Predictive performance of the clinical model, HNIS score, and combined model for major pathological response (MPR) across training, internal validation, and external validation cohorts.**

Cohort	Model	AUC (95% CI)	Sensitivity	Specificity	Accuracy	Brier score	Threshold
Training	Clinical model	0.611 (0.530-0.684)	0.598	0.596	0.597	0.242	0.514
Training	HNIS score	0.725 (0.655-0.788)	0.745	0.635	0.689	0.210	0.534
Training	Clinical + HNIS	0.745 (0.673-0.805)	0.863	0.548	0.704	0.204	0.409
Internal_Validation	Clinical model	0.569 (0.432-0.693)	0.618	0.529	0.574	0.246	0.514
Internal_Validation	HNIS score	0.736 (0.594-0.857)	0.765	0.676	0.721	0.206	0.534
Internal_Validation	Clinical + HNIS	0.729 (0.580-0.856)	0.882	0.618	0.750	0.209	0.409
External_Validation	Clinical model	0.554 (0.415-0.691)	0.467	0.605	0.544	0.249	0.514
External_Validation	HNIS score	0.753 (0.637-0.877)	0.600	0.711	0.662	0.200	0.534
External_Validation	Clinical + HNIS	0.719 (0.595-0.851)	0.733	0.526	0.618	0.214	0.409

AUC, area under the receiver operating characteristic curve; CI, confidence interval. The clinical model included age, sex, ECOG PS, cT stage, cN stage, PD-L1 CPS, MMR/MSI status, Lauren type, and differentiation. The HNIS model used the HNIS total score alone. The combined model included both. Models were derived in the training cohort and applied without re-fitting to the internal and external validation cohorts. The decision threshold was selected to maximize Youden's index in the training cohort and was applied unchanged to the validation cohorts. DeLong tests indicated significantly higher AUC for HNIS-based models compared with the clinical model in all three cohorts (all P<0.05); the combined model did not significantly outperform HNIS alone (DeLong P = 0.21-0.74).

single, inexpensive, blood-based composite, the Hormonal-Nutritional-Immune Score, provided clinically meaningful prediction of pathological response, severe immune-related toxicity, and long-term survival. Patients in the High-risk HNIS group were less than one-third as likely to achieve MPR as Low-risk patients (20.5% vs 67.4%; adjusted OR 0.13), nearly four times as likely to experience grade 3 or higher irAEs (26.5% vs 7.2%), and had markedly worse 3-year DFS (24.1% vs 69.6%) and OS (69.9% vs 94.9%). HNIS substantially outperformed a conventional clinical staging-based model for MPR prediction (training AUC 0.725 vs 0.611; external validation AUC 0.753 vs 0.554). To our knowledge, this is the first multidomain composite biomarker covering hormonal, nutritional, and inflammatory status to be developed and validated in a multicenter perioperative ICI cohort for LAGC, and it provides a reproducible framework for integrating endocrine, nutritional, and inflammatory information into pretreatment risk stratification.

The biological rationale for combining hormonal, nutritional, and inflammatory indicators is increasingly supported by mechanistic studies. Thyroid dysfunction is a recognized endocrine complication of immune checkpoint inhibition (18). Experimental studies link glucocorticoid signaling to impaired dendritic-cell function and dysfunctional CD8+ T-cell states in the tumor

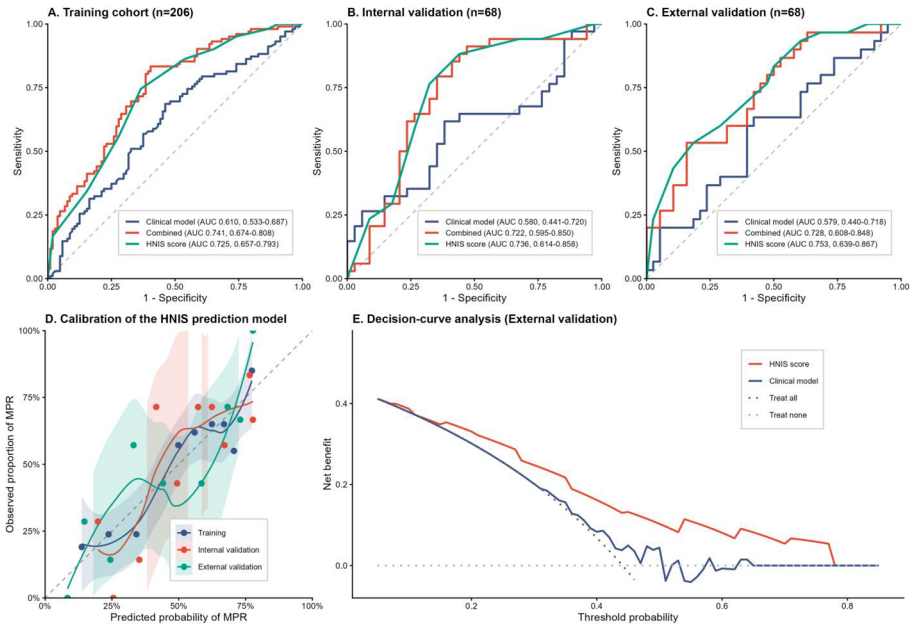

FIGURE 4
Performance of HNIS for prediction of major pathological response (MPR). **(A–C)** Receiver operating characteristic curves for the clinical model, the HNIS score, and the combined HNIS + clinical model in the **(A)** training, **(B)** internal validation, and **(C)** external validation cohorts. The HNIS-based models had higher AUC than the clinical model in all three cohorts (DeLong all P<0.05). **(D)** Calibration plot showing predicted versus observed MPR probabilities by deciles of predicted risk for the HNIS-based prediction model in the three cohorts; reasonable agreement is observed across deciles. **(E)** Decision-curve analysis showing higher net clinical benefit for the HNIS-based models across threshold probabilities of approximately 0.10 to 0.65 compared with treat-all, treat-none, and clinical-only strategies.

microenvironment (19, 40). PNI combines serum albumin and lymphocyte count, and low PNI has been associated with adverse clinical outcomes in gastrointestinal cancer (21, 22). NLR, SII, CRP, and CAR have prognostic associations in cancer, while local and systemic inflammatory responses can influence tumor progression and treatment outcomes (23–26). Single-marker associations have been described for each of these indicators in gastric and other cancers, but their combined effect has not been formally evaluated in the perioperative ICI setting. The component analyses support associations across all three domains, but several variables share measurements or strongly correlated information. In particular, CRP and CAR showed substantial overlap. LASSO and component-removal analyses therefore complement single-marker significance: a marker may be associated with outcome while adding little discrimination beyond the other components. The results support a pragmatic composite, not a claim that all 12 measurements have equal biological effects or are indispensable.

PD-L1 CPS and MSI-H/dMMR provide tumor-derived information relevant to ICI response in advanced gastric cancer. These biomarkers address different aspects of tumor biology and do not directly measure the endocrine, nutritional, or inflammatory abnormalities summarized by HNIS (10, 11). In our multivariable models, HNIS retained strong independent association with MPR after adjustment for PD-L1 CPS ≥5 and MMR/MSI-H status, and was an independent predictor of DFS and OS after adjusting for these and other tumor-intrinsic factors. The absolute AUC gain of approximately 0.20 from a clinical staging-only model (0.554-0.611 across cohorts) to HNIS-based prediction (0.725-0.753) is large for a clinical biomarker and exceeds the incremental discrimination reported for most existing pretreatment predictors of pathological response in LAGC. Importantly, HNIS is universally available, requires no specialized equipment or tissue, costs less than $20 per patient in routine clinical chemistry, and can be repeatedly measured to track patient state over time and during preoperative optimization.

Another notable finding was the inverse relationship between HNIS and irAEs: higher HNIS was associated with both higher rates of any-grade irAEs (51.8% vs 31.2% from High to Low risk) and grade 3 or higher irAEs (26.5% vs 7.2%). At first glance, this finding may appear counterintuitive, since patients with apparently more impaired baseline status had a higher rate of immune-mediated toxicity. Several mechanisms may explain this observation. First, ICI-induced loss of self-tolerance can result in endocrine toxicity, including thyroid dysfunction (18). Second, glucocorticoid signaling can promote dysfunctional CD8+ T-cell states in the tumor microenvironment (40), but its relationship to the observed toxicity gradient is not established by these data. Third, the same patients are more likely to require dose reductions, treatment delays, or complete withdrawal of PD-1 inhibitor, contributing to the lower rates of MPR observed in the High-risk group. From a clinical perspective, the combined association of HNIS with both reduced efficacy and increased toxicity has important implications: patients with high HNIS may benefit most from proactive endocrine and nutritional optimization, prophylactic monitoring, and intensified surveillance for irAEs. Whether such a preoperative optimization strategy can shift the response and toxicity balance is testable in a randomized window-of-opportunity trial.

Our results extend prior single-domain work in several important ways. Yao et al. examined TyG in an advanced gastric cancer cohort receiving sintilimab plus chemotherapy (20). That treatment setting and the reported cutoff differ from this neoadjuvant cohort, so the study does not validate the HNIS TyG threshold. PNI and SII have similarly been associated with prognosis in gastric cancer, but each captures only a fraction of the host immune and metabolic state (22, 33). HNIS summarizes baseline abnormalities across these domains. A high score is not itself an indication for thyroid hormone, vitamin D, statins, or metformin; individual abnormalities require assessment of their cause and usual clinical indications. The association analyses do not establish that correcting an HNIS component improves immunotherapy response. The reproducibility of HNIS in our external validation cohort, which was drawn from a different geographic region, supports the applicability of the score across Chinese tertiary centers, although broader validation in non-Asian populations and Western FLOT-dominant cohorts is essential before clinical adoption.

This study has several strengths. First, the multicenter design with 342 patients drawn from four geographically diverse Chinese tertiary centers provides external validity within the target population. Second, the fixed cutoffs and unweighted point structure make the score straightforward to calculate; the added analyses explicitly test the cost of this simplification. Third, the cohort included a representative mix of contemporary PD-1 inhibitors (sintilimab, camrelizumab, toripalimab, pembrolizumab, nivolumab) and chemotherapy backbones (SOX, XELOX, FLOT, and others), with no statistically detected treatment interaction in the added models; precision was limited for less frequently used agents. Fourth, central pathology adjudication using the Mandard TRG system, a median follow-up of 52.5 months, and a substantial number of survival events (DFS 202; OS 77) support reliable survival estimation. Fifth, by reporting AUC, calibration, Brier score, and decision-curve analysis across training, internal, and external validation cohorts, we provide a comprehensive assessment of model performance (39).

Several limitations should be acknowledged. First, the study is retrospective and observational, with the attendant risks of selection bias and unmeasured confounding despite extensive multivariable adjustment. Second, the original group boundaries were not proven optimal. The added weighted models did not improve internal discrimination, but some components were redundant for MPR and the resampling intervals are conditional on fitted models. The TyG and CAR boundaries are operational choices, and center-specific assay reference intervals were unavailable. Third, baseline biomarkers were measured within a 14-day window. The analytic dataset did not contain structured sampling-time infection status, recent corticosteroid exposure, nutritional intervention, or repeated pretreatment measurements. Infection, stress, tumor-related inflammation, bleeding, or a correctable nutritional deficit can influence several components simultaneously. The restricted-sample analyses address measured abnormalities but cannot establish their cause, temporal stability, or response to correction. Excluding low albumin alone would also remove part of the host phenotype that HNIS is designed to describe. Fourth, all patients were of Han Chinese ancestry from four Chinese tertiary centers; whether the HNIS framework and its cutoffs are portable to non-Chinese populations and to Western

perioperative cohorts using FLOT-dominant regimens warrants targeted validation. Fifth, although our cohort included GEJ adenocarcinoma, the relatively small number of GEJ cases (n=52, 15.2%) limits power for stratified GEJ-specific inference. The pembrolizumab and nivolumab subgroups and the 44 severe irAE events limit interaction precision; the heterogeneous "other chemotherapy" category is not a single regimen. Finally, the present analysis does not include tumor-microenvironment immunophenotyping or multi-omics validation, which would strengthen mechanistic interpretation; integration of HNIS with multimodal AI-based approaches (12–14, 41) is an attractive direction for future work.

Pending external prospective validation, the HNIS framework offers a low-cost, reproducible, and clinically interpretable adjunct to existing tumor biomarkers for stratifying patients with LAGC who are candidates for neoadjuvant PD-1 inhibitor plus chemotherapy. The ≥6 category identifies a group with less favorable observed outcomes in this cohort, but it is not a validated threshold for changing treatment. Continuous HNIS preserved more MPR discrimination than the tested groupings. Because every patient received immunochemotherapy, these data do not establish differential treatment benefit or a causal benefit from modifying score components.

Conclusions

In this multicenter retrospective cohort of 342 patients with locally advanced gastric or gastroesophageal junction adenocarcinoma receiving neoadjuvant PD-1 inhibitor plus platinum-based chemotherapy, a pretreatment Hormonal-Nutritional-Immune Score (HNIS) based on 12 routine blood-based indicators was an independent predictor of major pathological response, immune-related toxicity, disease-free survival, and overall survival. HNIS-based prediction outperformed a clinical staging-based model for MPR across training, internal validation, and external validation cohorts (AUCs 0.725 to 0.753 vs 0.554 to 0.611). HNIS is a simple, reproducible, and clinically interpretable biomarker that, pending prospective external validation in non-Chinese populations and in FLOT-dominant cohorts, has the potential to refine pretreatment risk stratification, identify patients who may benefit from preoperative endocrine and nutritional optimization, and support individualized neoadjuvant immunotherapy decisions for LAGC.

Data availability statement

The raw data supporting the conclusions of this article will be made available by the authors, without undue reservation.

Ethics statement

The study protocol was reviewed by the institutional review boards of all four hospitals, with the master ethics approval issued by the Fourth Hospital of Hebei Medical University (reference HEBMU-2024-IRB-031). The studies were conducted in accordance with the local legislation and institutional requirements. The ethics committee/institutional review board waived the requirement of written informed consent for participation from the participants or the participants' legal guardians/next of kin because this study was a multicenter retrospective observational analysis using only clinical, laboratory, pathological, treatment, and follow-up data that had already been generated during routine medical care. No additional intervention, examination, treatment modification, or biospecimen collection was performed, and the study posed no more than minimal risk to participants. All patient data were anonymized and de-identified before analysis, and no directly identifiable personal information was included in the research dataset. Because the study covered a relatively long time period and some patients were difficult to recontact, obtaining written informed consent from each individual participant was impracticable. Therefore, given the retrospective design, minimal risk, adequate privacy protection, and absence of adverse effects on patients' rights, safety, or welfare, the requirement for written informed consent was waived by the ethics committee.

Author contributions

ZW: Resources, Supervision, Writing – original draft, Writing – review & editing, Software, Validation. JZ: Writing – original draft, Resources, Project administration, Formal Analysis. LW: Validation, Methodology, Writing – original draft, Data curation. NM: Writing – original draft, Validation, Data curation, Methodology, Writing – review & editing. HG: Validation, Writing – review & editing, Supervision, Resources. YS: Investigation, Data curation, Writing – review & editing. WX: Investigation, Resources, Validation, Supervision, Writing – review & editing, Project administration. PY: Formal Analysis, Writing – review & editing, Methodology.

Funding

The author(s) declared that financial support was received for this work and/or its publication. This study was supported by the Hebei Provincial Medical Science Research Project Plan (20260919). The funders had no role in study design, data collection, analysis and interpretation, manuscript preparation, or the decision to submit for publication.

Acknowledgments

We thank the multidisciplinary tumor-board members at each participating center, the gastrointestinal pathologists who performed Mandard TRG adjudication, and the data managers and clinical research coordinators who supported retrospective data extraction. We are grateful to all patients and their families.

Conflict of interest

The author(s) declared that this work was conducted in the absence of any commercial or financial relationships that could be construed as a potential conflict of interest.

Generative AI statement

The author(s) declared that generative AI was not used in the creation of this manuscript.

Any alternative text (alt text) provided alongside figures in this article has been generated by Frontiers with the support of artificial intelligence and reasonable efforts have been made to ensure accuracy, including review by the authors wherever possible. If you identify any issues, please contact us.

Publisher's note

All claims expressed in this article are solely those of the authors and do not necessarily represent those of their affiliated organizations, or those of the publisher, the editors and the reviewers. Any product that may be evaluated in this article, or claim that may be made by its manufacturer, is not guaranteed or endorsed by the publisher.

Supplementary material

The Supplementary Material for this article can be found online at: https://www.frontiersin.org/articles/10.3389/fimmu.2026.1875198/full#supplementary-material

References

1. Sung H, Ferlay J, Siegel RL, Laversanne M, Soerjomataram I, Jemal A, et al. Global cancer statistics 2020: GLOBOCAN estimates of incidence and mortality worldwide for 36 cancers in 185 countries. *CA Cancer J Clin*. (2021) 71:209–49. doi: 10.3322/caac.21660

2. Wang FH, Zhang XT, Tang L, Wu Q, Cai MY, Li YF, et al. The Chinese Society of Clinical Oncology (CSCO): Clinical guidelines for the diagnosis and treatment of gastric cancer, 2023. *Cancer Commun (Lond)*. (2024) 44:127–72. doi: 10.1002/cac2.12516

3. Smyth EC, Nilsson M, Grabsch HI, van Grieken NC, Lordick F. Gastric cancer. *Lancet*. (2020) 396:635–48. doi: 10.1016/s0140-6736(20)31288-5

4. Al-Batran SE, Homann N, Pauligk C, Goetze TO, Meiler J, Kasper S, et al. Perioperative chemotherapy with fluorouracil plus leucovorin, oxaliplatin, and docetaxel versus fluorouracil or capecitabine plus cisplatin and epirubicin for locally advanced, resectable gastric or gastro-oesophageal junction adenocarcinoma (FLOT4): a randomised, phase 2/3 trial. *Lancet*. (2019) 393:1948–57. doi: 10.1016/s0140-6736(18)32557-1

5. Zhang X, Liang H, Li Z, Xue Y, Wang Y, Zhou Z, et al. Perioperative or postoperative adjuvant oxaliplatin with S-1 versus adjuvant oxaliplatin with capecitabine in patients with locally advanced gastric or gastro-oesophageal junction adenocarcinoma undergoing D2 gastrectomy (RESOLVE): an open-label, superiority and non-inferiority, phase 3 randomised controlled trial. *Lancet Oncol*. (2021) 22:1081–92. doi: 10.1016/s1470-2045(21)00297-7

6. Lorenzen S, Götze TO, Thuss-Patience P, Biebl M, Homann N, Schenk M, et al. Perioperative atezolizumab plus fluorouracil, leucovorin, oxaliplatin, and docetaxel for resectable esophagogastric cancer: interim results from the randomized, multicenter, phase II/III DANTE/IKF-s633 trial. *J Clin Oncol*. (2024) 42:410–20. doi: 10.1200/jco.23.00975

7. Janjigian YY, Al-Batran SE, Wainberg ZA, Muro K, Molena D, Van Cutsem E, et al. Perioperative durvalumab in gastric and gastroesophageal junction cancer. *N Engl J Med*. (2025) 393:217–30. doi: 10.1056/nejmoa2503701

8. Shitara K, Rha SY, Wyrwicz LS, Oshima T, Karaseva N, Osipov M, et al. Neoadjuvant and adjuvant pembrolizumab plus chemotherapy in locally advanced gastric or gastro-oesophageal cancer (KEYNOTE-585): an interim analysis of the multicentre, double-blind, randomised phase 3 study. *Lancet Oncol*. (2024) 25:212–24. doi: 10.1016/s1470-2045(23)00541-7

9. Becker K, Mueller JD, Schulmacher C, Ott K, Fink U, Busch R, et al. Histomorphology and grading of regression in gastric carcinoma treated with neoadjuvant chemotherapy. *Cancer*. (2003) 98:1521–30. doi: 10.1002/cncr.11660

10. Marabelle A, Le DT, Ascierto PA, Di Giacomo AM, De Jesus-Acosta A, Delord JP, et al. Efficacy of pembrolizumab in patients with noncolorectal high microsatellite instability/mismatch repair-deficient cancer: results from the phase II KEYNOTE-158 study. *J Clin Oncol*. (2020) 38:1–10. doi: 10.1200/jco.19.02105

11. Janjigian YY, Shitara K, Moehler M, Garrido M, Salman P, Shen L, et al. First-line nivolumab plus chemotherapy versus chemotherapy alone for advanced gastric, gastro-oesophageal junction, and oesophageal adenocarcinoma (CheckMate 649): a randomised, open-label, phase 3 trial. *Lancet*. (2021) 398:27–40. doi: 10.1016/s0140-6736(21)00797-2

12. Ding P, Yang J, Guo H, Wu J, Wu H, Li T, et al. Multimodal artificial intelligence-based virtual biopsy for diagnosing abdominal lavage cytology-positive gastric cancer. *Adv Sci (Weinh)*. (2025) 12:e2411490. doi: 10.1002/advs.202411490

13. Ding P, Yang J, Chen S, Guo H, Wu J, Wu H, et al. Interpretable multimodal fusion model enhances postoperative recurrence prediction in gastric cancer. *Adv Sci (Weinh)*. (2025) 12:e08190. doi: 10.1002/advs.202508190

14. Ding PA, Yang S, Meng LJ, Chen S, Li SP, Guo HH, et al. A multimodal deep learning model for preoperative prediction of post-operative complications in gastric cancer. *Ann Oncol*. (2026) 37:1423–36. doi: 10.1016/j.annonc.2026.07.004

15. Ding P, Yang J, Guo H, Chen S, Liu Y, Han X, et al. Multimodal radiopathomics model predicts postoperative metachronous liver metastasis in gastric cancer. *Nat Commun*. (2026) 17:10518. doi: 10.1038/s41467-026-76382-x

16. Hegde PS, Chen DS. Top 10 challenges in cancer immunotherapy. *Immunity*. (2020) 52:17–35. doi: 10.1016/j.immuni.2019.12.011

17. Spranger S, Gajewski TF. Mechanisms of tumor cell-intrinsic immune evasion. *Annu Rev Cancer Biol*. (2018) 2:213–28. doi: 10.1146/annurev-cancerbio-030617-050606

18. Stelmachowska-Banaś M, Czajka-Oraniec I. Management of endocrine immune-related adverse events of immune checkpoint inhibitors: an updated review. *Endocr Connect*. (2020) 9:R207–28. doi: 10.1530/ec-20-0342

19. Yang H, Xia L, Chen J, Zhang S, Martin V, Li Q, et al. Stress-glucocorticoid-TSC22D3 axis compromises therapy-induced antitumor immunity. *Nat Med*. (2019) 25:1428–41. doi: 10.1038/s41591-019-0566-4

20. Yao ZY, Ma X, Cui YZ, Liu J, Han ZX, Song J. Impact of triglyceride-glucose index on the long-term prognosis of advanced gastric cancer patients receiving immunotherapy combined with chemotherapy. *World J Gastroenterol*. (2025) 31:102249. doi: 10.3748/wjg.v31.i5.102249

21. Onodera T, Goseki N, Kosaki G. Prognostic nutritional index in gastrointestinal surgery of malnourished cancer patients. *Nihon Geka Gakkai Zasshi*. (1984) 85:1001–5

22. Maejima K, Taniai N, Yoshida H. The prognostic nutritional index as a predictor of gastric cancer progression and recurrence. *J Nippon Med Sch*. (2022) 89:487–93. doi: 10.1272/jnms.jnms.2022_89-507

23. Hu B, Yang XR, Xu Y, Sun YF, Sun C, Guo W, et al. Systemic immune-inflammation index predicts prognosis of patients after curative resection for hepatocellular carcinoma. *Clin Cancer Res*. (2014) 20:6212–22. doi: 10.1158/1078-0432.ccr-14-0442

24. Templeton AJ, McNamara MG, Šeruga B, Vera-Badillo FE, Aneja P, Ocaña A, et al. Prognostic role of neutrophil-to-lymphocyte ratio in solid tumors: a systematic review and meta-analysis. *J Natl Cancer Inst*. (2014) 106:dju124. doi: 10.1093/jnci/dju124

25. Diakos CI, Charles KA, McMillan DC, Clarke SJ. Cancer-related inflammation and treatment effectiveness. *Lancet Oncol*. (2014) 15:e493–503. doi: 10.1016/s1470-2045(14)70263-3

26. Mao M, Wei X, Sheng H, Chi P, Liu Y, Huang X, et al. C-reactive protein/albumin and neutrophil/lymphocyte ratios and their combination predict overall survival in patients with gastric cancer. *Oncol Lett*. (2017) 14:7417–24. doi: 10.3892/ol.2017.7179

27. Zou Y, Wang D, Cheng X, et al. Reference intervals for thyroid-associated hormones and the prevalence of thyroid diseases in the Chinese population. *Ann Lab Med*. (2021) 41:77–85. doi: 10.3343/alm.2021.41.1.77

28. Li Y, Shan Z, Teng W, et al. Estimated change in prevalence of abnormal thyroid-stimulating hormone levels in China according to the application of the kit-recommended or NACB standard reference interval. *EClinicalMedicine*. (2021) 32:100723. doi: 10.1016/j.eclinm.2021.100723

29. American College of Physicians. Reference ranges (2026). Available online at: https://annualmeeting.acponline.org/educational-program/reference-ranges. (Accessed October 29, 2026)

30. Jiang X, Hiki N, Nunobe S, et al. Prognostic importance of the inflammation-based Glasgow prognostic score in patients with gastric cancer. *Br J Cancer*. (2012) 107:275–9. doi: 10.1038/bjc.2012.262

31. Liu X, Qiu H, Huang Y, et al. Impact of preoperative anemia on outcomes in patients undergoing curative resection for gastric cancer: a single-institution retrospective analysis of 2163 Chinese patients. *Cancer Med*. (2018) 7:360–9. doi: 10.1002/cam4.1309

32. Mohri Y, Tanaka K, Toiyama Y, et al. Impact of preoperative neutrophil to lymphocyte ratio and postoperative infectious complications on survival after curative gastrectomy for gastric cancer: a single institutional cohort study. *Med (Baltimore)*. (2016) 95:e3125. doi: 10.1097/md.0000000000003125

33. Chen L, Yan Y, Zhu L, et al. Systemic immune-inflammation index as a useful prognostic indicator predicts survival in patients with advanced gastric cancer treated with neoadjuvant chemotherapy. *Cancer Manag Res*. (2017) 9:849–67. doi: 10.2147/cmar.s151026

34. Holick MF, Binkley NC, Bischoff-Ferrari HA, et al. Evaluation, treatment, and prevention of vitamin D deficiency: an Endocrine Society clinical practice guideline. *J Clin Endocrinol Metab*. (2011) 96:1911–30. doi: 10.1210/jc.2011-0385

35. Demay MB, Pittas AG, Bikle DD, et al. Vitamin D for the prevention of disease: an Endocrine Society clinical practice guideline. *J Clin Endocrinol Metab*. (2024) 109:1907–47. doi: 10.1210/clinem/dgae290

36. Gu L, Wang M, Cui X, et al. Clinical significance of peripheral blood-derived inflammation markers in advanced gastric cancer after radical resection. *BMC Surg*. (2020) 20:219. doi: 10.1186/s12893-020-00884-8

37. DeLong ER, DeLong DM, Clarke-Pearson DL. Comparing the areas under two or more correlated receiver operating characteristic curves: a nonparametric approach. *Biometrics*. (1988) 44:837–47. doi: 10.2307/2531595

38. Steyerberg EW, Vickers AJ, Cook NR, Gerds T, Gonen M, Obuchowski N, et al. Assessing the performance of prediction models: a framework for traditional and novel measures. *Epidemiology*. (2010) 21:128–38. doi: 10.1097/ede.0b013e3181c30fb2

39. Vickers AJ, Elkin EB. Decision curve analysis: a novel method for evaluating prediction models. *Med Decis Making*. (2006) 26:565–74. doi: 10.1177/0272989x06295361

40. Acharya N, Madi A, Zhang H, Klapholz M, Escobar G, Dulberg S, et al. Endogenous glucocorticoid signaling regulates CD8+ T cell differentiation and development of dysfunction in the tumor microenvironment. *Immunity*. (2020) 53:658–671.e6. doi: 10.1016/j.immuni.2020.08.005

41. Ding P, Chen S, Guo H, Yang S, Wang X, Han X, et al. A deep learning-based digital biopsy for predicting early recurrence in gastric cancer. *Nat Commun*. (2026) 17:5220. doi: 10.1038/s41467-026-71347-6